

# Minimization of Delay and Crosstalk in High-Speed VLSI Interconnects

Qi-jun Zhang, *Member, IEEE*, Stephen Lum, *Member, IEEE*, and Michel S. Nakhla, *Senior Member, IEEE*

**Abstract**—This paper presents design optimization of time responses of high-speed VLSI interconnects modeled by distributed coupled transmission line networks. The problem of simultaneous minimization of crosstalk, delay and reflection is formulated into minimax optimization. Design variables include physical/geometrical parameters of the interconnects and parameters in terminating/matching networks. A recently published simulation and sensitivity analysis technique for multiconductor transmission lines is expanded to directly address the VLSI interconnect environment. The new approach permits efficient physical/geometrical oriented interconnect design using exact gradient based minimax optimization. Examples of interconnect optimization demonstrate significant reductions of crosstalk, delay, distortion and reflection at all vital connection ports. The technique developed is an important step towards optimal design of circuit interconnects for high-speed digital computers and communication systems.

## I. INTRODUCTION

THE STUDY of time-domain responses of VLSI interconnect networks is instrumental in the design of high-speed digital computers and communication systems. Improperly designed interconnects can result in increased signal delay, ringing, reflection and false switching. With subnanosecond rise times, the electrical length of interconnects can become a significant fraction of a wavelength. Consequently the conventional lumped impedance model is not adequate in this case. Instead a distributed transmission line model should be used. This problem has attracted the attention of many researchers. Several techniques have been proposed in the literature for the analysis of VLSI interconnects and coupled microstrip lines, e.g., [1]–[13].

An intuitive solution to the problem of delay and reflections is to decrease the length of the interconnections by increasing the system density. The trend toward greater density, however, fosters another problem, that of crosstalk between adjacent transmission lines. A designer must make proper trade-offs between various conflicting factors. For large circuits the relation between a large number of circuit parameters and design criteria becomes ex-

Manuscript received September 10, 1991; revised February 5, 1992. This work was supported through the Computer-Aided Engineering Chairs funded by Bell-Northern Research and the Natural Sciences and Engineering Research Council of Canada.

Q. J. Zhang and M. S. Nakhla are with the Department of Electronics, Carleton University, Ottawa, Canada K1S 5B6.

S. Lum is with Bell-Northern Research Ltd., Ottawa, Canada K1Y 4H7. IEEE Log Number 9108317.

tremely complicated. There is an increasing need of a design optimization approach that uses interconnect parameters explicitly in overall network design, a problem not yet adequately treated in the literature.

The immediate difficulty in pursuing such a direction is that most of the existing simulation techniques do not provide sensitivities. Since the simulation of distributed multiconductor transmission lines is much more complicated than typical lumped elements, e.g., an eigenvalue problem has to be solved, non-gradient based optimization will be extremely CPU intensive for realistic networks containing many multiconductor transmission line elements. Increased computational effort is also due to the nature of time-domain simulations. In conventional integration or FFT based simulators, responses at a time point depend upon the solutions of responses at other time points. Therefore, the entire time waveform has to be calculated even if the response to be optimized is only in a time subinterval. This phenomenon does not exist in frequency-domain optimization, since circuit responses at any frequency can be computed independently.

The recent availability of sensitivity analysis based on numerical inversion of Laplace transform (NILT) for lossy coupled transmission lines [2] motivated us to pursue time-domain optimization of VLSI interconnect networks. The problem of simultaneous minimization of crosstalk, delay and reflection is formulated into a minimax problem. Design variables include physical/geometrical parameters of the interconnects and parameters in the termination/matching networks. Exact sensitivity information of time responses of the network with respect to design variables is used with a powerful two stage minimax optimization. Our NILT based network simulation decouples the dependence between responses at different time points, enhancing the efficiency of time-domain optimization. In our example with 25 transmission lines, 61 error functions and 27 design variables, a substantial reduction of crosstalk, delay, distortion and reflection at several vital connection ports was simultaneously achieved.

In Section II, simulation and sensitivity analysis of lossy coupled transmission lines using the NILT technique is summarized. The technique is expanded to efficiently handle physical/geometrical variables and to exploit common parameters between different circuit elements in VLSI interconnect networks. In Section III,

time-domain specifications are described for crosstalk, delay, rise/fall times and signal reflection. The design problem is formulated into minimax optimization. Two numerical examples are presented in Section IV, illustrating the principles of time-domain interconnect optimization.

## II. NILT SIMULATION AND SENSITIVITY ANALYSIS

The NILT simulation and sensitivity analysis for multiconductor transmission lines are described in detail in [1], [2]. In this section, the technique is summarized and expanded to directly address the VLSI interconnect design environment. The expanded approach efficiently handles physical/geometrical design variables and the large number of repeating parameters typically exist in VLSI interconnect circuits.

### Analysis of Multiconductor Transmission Lines [1]

Distributed multiconductor transmission line models are used as the basic elements for VLSI interconnect networks. The transmission line model is assumed to be uniform along its length with an arbitrary cross section. The cross section of transmission line  $k$  with  $N_k$  signal conductors, can be represented by the following  $N_k \times N_k$  matrices of line parameters: the inductance per unit length  $\mathbf{L}$ , the resistance per unit length  $\mathbf{R}$ , the capacitance per unit length  $\mathbf{C}$ , and the conductance per unit length  $\mathbf{G}$ . These matrix parameters are computed from physical/geometrical parameters using either quasi-static analysis [14], [15] or empirical formulas [16].

Let  $\gamma_i^2$  be an eigenvalue of the matrix  $\mathbf{Z}_L \mathbf{Y}_L$  with an associated eigenvector  $\mathbf{x}_i$ , where  $\mathbf{Z}_L = \mathbf{R} + s\mathbf{L}$  and  $\mathbf{Y}_L = \mathbf{G} + s\mathbf{C}$ , i.e.,

$$(\gamma_i^2 \mathbf{U} - \mathbf{Z}_L \mathbf{Y}_L) \mathbf{x}_i = 0 \quad (1)$$

where  $\mathbf{U}$  is the identity matrix and  $s$  is the complex frequency.

The admittance matrix for the multiconductor transmission line is

$$\mathbf{A}_k = \begin{bmatrix} \mathbf{S}_i \mathbf{E}_1 \mathbf{S}_v^{-1} & \mathbf{S}_i \mathbf{E}_2 \mathbf{S}_v^{-1} \\ \mathbf{S}_i \mathbf{E}_2 \mathbf{S}_v^{-1} & \mathbf{S}_i \mathbf{E}_1 \mathbf{S}_v^{-1} \end{bmatrix} \quad (2)$$

where

$$\mathbf{E}_1 = \text{diag} \{(1 + e^{-2\gamma_i l}) / (1 - e^{-2\gamma_i l}), i = 1, 2, \dots, N_k\} \quad (3)$$

$$\mathbf{E}_2 = \text{diag} \{2 / (e^{-\gamma_i l} - e^{\gamma_i l}), i = 1, 2, \dots, N_k\}, \quad (4)$$

where  $l$  is the length of the transmission line.  $\mathbf{S}_v$  is a matrix containing all eigenvectors  $\mathbf{x}_i$ ,  $i = 1, 2, \dots, N_k$ .  $\Gamma$  is a diagonal matrix with  $\Gamma_{i,i} = \gamma_i$ , and  $\mathbf{S}_i = \mathbf{Z}_L^{-1} \mathbf{S}_v \Gamma$ .

### Modified Nodal Equations for a VLSI Interconnect Network

Suppose the overall network  $\pi$  consists of lumped elements and  $N_s$  subnetworks. In this paper a typical sub-

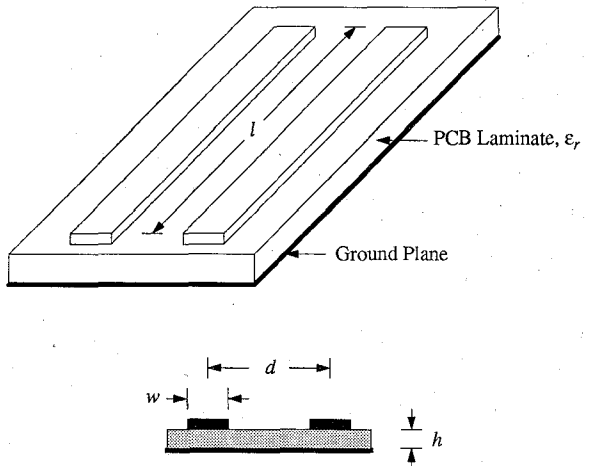


Fig. 1. Physical/geometrical parameters of a 2-conductor transmission line.

work represents a distributed multiconductor transmission line. Suppose these subnetworks are arranged into  $N_g$  groups. Within the same group, different transmission lines have the same cross-sectional geometry and the same material parameters, but different lengths. Fig. 1 shows the physical layout and the cross-sectional view of a 2-conductor transmission line on a printed circuit board (PCB). Let  $I_i$ ,  $i = 1, 2, \dots, N_g$ , be an index set defined as

$$I_i = \{k \mid \text{transmission line } k \text{ belongs to group } i, k = 1, 2, \dots, N_s\}. \quad (5)$$

The modified nodal equations [17] for the overall network  $\pi$  is

$$\mathbf{C}_\pi \frac{d\mathbf{v}_\pi(t)}{dt} + \mathbf{G}_\pi \mathbf{v}_\pi(t) + \sum_{i=1}^{N_g} \sum_{k \in I_i} \mathbf{D}_k \mathbf{i}_k(t) = \mathbf{e}_\pi(t) \quad (6)$$

where  $\mathbf{C}_\pi$  and  $\mathbf{G}_\pi$  are  $N_\pi$  by  $N_\pi$  matrices determined by lumped elements in the network.  $\mathbf{v}_\pi(t)$  is the vector of node voltage waveforms appended by independent voltage source currents and inductor current waveforms.  $\mathbf{D}_k$  is a  $N_\pi$  by  $2N_k$  incidence matrix containing 1's and 0's, which maps the  $2N_k$ -terminals of the transmission line into the  $N_\pi$ -node space of the network  $\pi$ .  $\mathbf{i}_k(t)$  is the terminal current waveform of the  $k$ th distributed transmission line and  $\mathbf{e}_\pi(t)$  is the vector of source waveforms.

The  $s$ -domain equation is obtained by taking the Laplace transform of (6)

$$\mathbf{Y}_\pi \mathbf{V}_\pi(s) = \mathbf{E}_\pi(s) + \mathbf{C}_\pi \mathbf{v}_\pi(0) \quad (7)$$

where

$$\mathbf{Y}_\pi = \mathbf{G}_\pi + s\mathbf{C}_\pi + \sum_{i=1}^{N_g} \sum_{k \in I_i} \mathbf{D}_k \mathbf{A}_k \mathbf{D}_k^T \quad (8)$$

where  $\mathbf{A}_k$  is the nodal admittance matrix of the  $k$ th distributed transmission line. The eigenvalue problem (1) can be solved only once for each group of transmission lines  $I_i$ . Individual  $\mathbf{A}_k$  within the same group can be obtained using (2)–(4).

### Numerical Inversion of Laplace Transform [1]

The method used for circuit simulation and sensitivity analysis is based on the NILT technique [1], [2]. We solve the circuit in the s-domain to obtain nodal voltages  $V_\pi(s)$ . The transient voltages  $\mathbf{v}_\pi(t)$  are obtained through numerical Laplace inversion, i.e.,

$$\mathbf{v}_\pi(t) = -(1/t) \sum_{i=1}^{M'} \text{Real} [K_i V_\pi(z_i/t)] \quad (9)$$

where  $z_i$  and  $K_i$ ,  $i = 1, 2, \dots, M'$ , are predetermined poles and residues of a Padé rational function approximating  $e^z$  [1].

From (9) it can be seen that the response at time  $t$  can be obtained without calculating the response at any other time points. This is particularly well suited to design optimization since specifications are typically imposed on time subintervals.

### Exact Sensitivity Calculation

Suppose  $\phi$  is a design variable. Let

$$v_{\text{out}}(t) = \mathbf{u}^T \mathbf{v}_\pi(t) \quad (10)$$

be the response of interest, where  $\mathbf{u}$  is a constant  $N_\pi$ -vector. Using the NILT technique, the sensitivity of time-domain response  $v_{\text{out}}(t)$  with respect to  $\phi$  is obtained from frequency-domain sensitivity  $\partial V_{\text{out}}(s)/\partial\phi$  through

$$\partial v_{\text{out}}(t)/\partial\phi = -(1/t) \sum_{i=1}^{M'} \text{Real} [K_i \partial V_{\text{out}}(z_i/t)/\partial\phi]. \quad (11)$$

When  $\phi$  is a parameter in lumped elements,  $\partial V_{\text{out}}(s)/\partial\phi$  is computed using the exact adjoint sensitivity technique [18]. When  $\phi$  is a transmission line parameter, the computation is more involved. We first compute the sensitivities of the eigenvalues  $\gamma_i^2$  and eigenvectors  $\mathbf{x}_i$  with respect to the variable  $\phi$  by solving the linear equation

$$\begin{bmatrix} \gamma_i^2 \mathbf{U} - \mathbf{Z}_L \mathbf{Y}_L & \mathbf{x}_i \\ \mathbf{x}_i^T & 0 \end{bmatrix} \begin{bmatrix} \partial \mathbf{x}_i / \partial \phi \\ \partial \gamma_i^2 / \partial \phi \end{bmatrix} = \begin{bmatrix} [\partial(\mathbf{Z}_L \mathbf{Y}_L)/\partial\phi] \mathbf{x}_i \\ 0 \end{bmatrix}. \quad (12)$$

This equation can be solved only once for each group of transmission lines. For individual members in the same group, we calculate sensitivities of matrices  $\mathbf{E}_1$  and  $\mathbf{E}_2$ . From this information, the sensitivity of the transmission line matrix  $\mathbf{A}_k$  is computed using

$$\begin{aligned} \partial \mathbf{A}_k / \partial \phi = & \begin{bmatrix} (\partial \mathbf{S}_i / \partial \phi) \mathbf{E}_1 \mathbf{S}_v^{-1} & (\partial \mathbf{S}_i / \partial \phi) \mathbf{E}_2 \mathbf{S}_v^{-1} \\ (\partial \mathbf{S}_i / \partial \phi) \mathbf{E}_2 \mathbf{S}_v^{-1} & (\partial \mathbf{S}_i / \partial \phi) \mathbf{E}_1 \mathbf{S}_v^{-1} \end{bmatrix} \\ & + \begin{bmatrix} \mathbf{S}_i (\partial \mathbf{E}_1 / \partial \phi) \mathbf{S}_v^{-1} & \mathbf{S}_i (\partial \mathbf{E}_2 / \partial \phi) \mathbf{S}_v^{-1} \\ \mathbf{S}_i (\partial \mathbf{E}_2 / \partial \phi) \mathbf{S}_v^{-1} & \mathbf{S}_i (\partial \mathbf{E}_1 / \partial \phi) \mathbf{S}_v^{-1} \end{bmatrix} \\ & - \mathbf{A}_k \text{diag} \{ \partial \mathbf{S}_v / \partial \phi \} \mathbf{S}_v^{-1}, \quad (\partial \mathbf{S}_v / \partial \phi) \mathbf{S}_v^{-1} \}. \end{aligned} \quad (13)$$

If  $\phi$  is a cross-sectional geometrical parameter or a material parameter in transmission line group  $I_i$ , the sensitivity is

$$\partial V_{\text{out}}(s)/\partial\phi = -(\mathbf{V}_\pi^a)^T \left[ \sum_{k \in I_i} \mathbf{D}_k (\partial \mathbf{A}_k / \partial \phi) \mathbf{D}_k^T \right] \mathbf{V}_\pi \quad (14)$$

where  $\mathbf{V}_\pi^a$  is the adjoint voltage vector solved from

$$\mathbf{Y}_\pi^T \mathbf{V}_\pi^a = \mathbf{u}. \quad (15)$$

If  $\phi$  is the length of transmission line  $k$ , the sensitivity is

$$\partial V_{\text{out}}(s)/\partial\phi = -(\mathbf{V}_\pi^a)^T \mathbf{D}_k (\partial \mathbf{A}_k / \partial \phi) \mathbf{D}_k^T \mathbf{V}_\pi. \quad (16)$$

Compared to the original technique in [1], [2], the new approach provides enhanced efficiency in both simulation and sensitivity analysis by using fewer eigenvalue evaluations. It hierarchically utilizes parameters at the element level and the transmission line group level during sensitivity evaluation. In addition this approach eliminates many repeating variables and equality constraints that are otherwise needed in formulating optimization.

### Sensitivity with Respect to Physical/Geometrical Parameters

The number of physical/geometrical parameters for a multiconductor transmission line is much smaller than the number of its electrical parameters. For example a 4-conductor transmission line has 65 electrical parameters ( $\mathbf{R}$ ,  $\mathbf{L}$ ,  $\mathbf{C}$ ,  $\mathbf{G}$  matrices and length  $l$ ) and only 10 physical/geometrical parameters (widths of 4 conductors, distance between adjacent conductors, conductor length, PCB height, dielectric constant). Therefore efficient optimization should bypass the evaluation of derivatives of response  $V_{\text{out}}(s)$  with respect to the transmission line matrices  $\mathbf{R}$ ,  $\mathbf{L}$ ,  $\mathbf{G}$  and  $\mathbf{C}$ . Physical/geometrical parameters should be directly used as the variables for the differentiation of the right-hand-side of (12).

## III. FORMULATION OF OPTIMIZATION

Optimization has been used in design, modelling, tuning, diagnosis and yield optimization problems [19]–[24]. Frequency-domain based optimization has been widely used. In this section we describe a systematic formulation for optimization of transient responses such as delay, rise/fall times, crosstalk and reflection as required in high-speed VLSI interconnect design.

### Formulation of Error Functions

Consider a VLSI interconnect network excited by a trapezoidal signal. Let  $T$  be the signal duration between the time when the trapezoidal signal triggers a switch-on state and the time when it triggers a switch-off state. Let  $\phi$  be a vector of design variables. Let  $v_j(\phi, t)$  be the response signal at node  $j$  and time  $t$ . Suppose  $J_1$  is an index set containing all nodes of interest at which the desired response is a signal corresponding to the excitation. Let  $J_2$  be an index set containing all nodes of interest at which

the desired response is zero. In other words, node  $j$ ,  $j \in J_1$ , is on the path of the signal propagation from the source excitation. Node  $j$ ,  $j \in J_2$ , is not on the path of signal propagation. Let  $w_d$ ,  $w_f$ ,  $w_c$  and  $w_r$  denote positive weighting factors.

Suppose the signal propagation delay is described by the time at which the transient signal reaches a threshold value  $v_T$ . Let  $\tau_{j,\max}$  be the upper specification for the propagation delay at node  $j$ . The error function for delay minimization can be equivalently described by

$$-w_d(v_j(\phi, \tau_{j,\max}) - v_T) \quad \text{for } j \in J_1. \quad (17)$$

Suppose  $\tau_j$  is the desired delay value. To locate the signal to be exactly or almost exactly at this desired time, we define two error functions

$$w_d(v_j(\phi, \tau_j) - v_T) \quad (18a)$$

and

$$-w_d(v_j(\phi, \tau_j) - v_T) \quad \text{for } j \in J_1. \quad (18b)$$

Due to transmission line effects, a response signal may rise/fall much more slowly than the source signal does. Suppose the required rise time is  $t_r$  during which the signal should rise from below threshold  $v_{T,\text{low}}$  to above  $v_{T,\text{high}}$ . The following two error functions are used

$$w_f(v_j(\phi, \tau_j - \alpha t_r) - v_{T,\text{low}}) \quad (19a)$$

and

$$-w_f(v_j(\phi, \tau_j + \beta t_r) - v_{T,\text{high}}) \quad \text{for } j \in J_1 \quad (19b)$$

where  $\alpha$  and  $\beta$  are positive and  $\alpha + \beta = 1$ .

Suppose the required fall time is  $t_f$  during which the signal should fall from above  $v_{T,\text{high}}$  to below  $v_{T,\text{low}}$ . The following two error functions are used

$$w_f(v_j(\phi, \tau_j + T + \lambda t_f) - v_{T,\text{low}}) \quad (20a)$$

and

$$-w_f(v_j(\phi, \tau_j + T - \mu t_f) - v_{T,\text{high}}) \quad \text{for } j \in J_1 \quad (20b)$$

where  $\lambda$  and  $\mu$  are positive and  $\lambda + \mu = 1$ .

The existence of undesired signal at node  $j$ ,  $j \in J_2$ , is due to coupling between the multiconductors. Suppose  $S_{cj}(t)$  denotes the upper specification on the magnitude of crosstalk at node  $j$  and time  $t$ ,  $0 < t < \infty$ . We select several time samples  $t_i$ ,  $i = 1, 2, \dots$ , in the interval  $0 < t_i < \infty$  and at each sample point define two error functions

$$w_c(v_j(\phi, t_i) - S_{cj}(t_i)) \quad (21a)$$

and

$$-w_c(v_j(\phi, t_i) + S_{cj}(t_i)) \quad \text{for } j \in J_2 \text{ and } 0 < t_i < \infty. \quad (21b)$$

Since the source signal is of duration  $T$ , an ideal response should vanish after  $t = T + \tau_j + \delta$ , where  $\delta$  is a small value not exceeding  $t_f$ . But due to reflections and

undesired ringing, the signal may continue to exist for an extended period of time. Suppose  $S_{rj}(t)$  is the upper specification on the magnitude of signal reflections at node  $j$  and time  $t$ ,  $T + \tau_j + \delta < t < \infty$ . For each time sample  $t_i$  selected in the interval  $T + \tau_j + \delta < t_i < \infty$  we define two error functions

$$w_r(v_j(\phi, t_i) - S_{rj}(t_i)) \quad (22a)$$

and

$$-w_r(v_j(\phi, t_i) + S_{rj}(t_i)) \quad \text{for } j \in J_1 \text{ and } T + \tau_j + \delta < t_i < \infty. \quad (22b)$$

The various specifications are illustrated in Fig. 2.

### Selection of Optimization Variables

The overall circuit performance is affected by parameters in both the interconnections and their terminations. The terminations typically represent basic VLSI circuit blocks and matching networks. The parameters in the termination/matching networks are considered optimizable. For interconnect parameters, we consider the physical/geometrical parameters of the transmission lines as shown in Fig. 1. In practice there are two stages of interconnect design. In the first stage, the length of the transmission line  $l$ , the distance between the coupled conductors  $d$ , and the width of the conductors  $w$  can be optimized. The thickness of PCB layer  $h$  is typically selected from a set of standard values. In the second design stage only the length  $l$  is optimizable.

### Constraints for Optimization

Design variables must be subject to design rules. Simple lower and upper bounds on variables should be applied according to design profile. Conflicting factors in design are also due to additional constraints. For example, the total length of several interconnect lines must be limited by the physical dimensions of the circuit chip and/or the PCB. In this case, shortening an interconnect will make another interconnect longer. The total separation between several coupled conductors must be constrained by the geometrical space available to them. In this case to reduce coupling by distancing a pair of conductors will force other conductors to be closer.

### Formulation of Optimization

Let  $e(\phi)$  be a vector containing all necessary error functions as defined in (17)–(22). Let  $m$  be the total number of such error functions. Let  $U(\phi)$  be the maximum of all error functions  $e_j(\phi)$ ,  $j = 1, 2, \dots, m$ , i.e.,

$$U(\phi) \triangleq \max_j \{e_j(\phi)\}. \quad (23)$$

If several specifications such as those on delay, crosstalk and reflections are simultaneously violated,  $U(\phi)$  represents the largest weighted violation. The design optimization problem is to find  $\phi$  such that

$$\underset{\phi}{\text{minimize}} \quad U(\phi) \quad (24a)$$

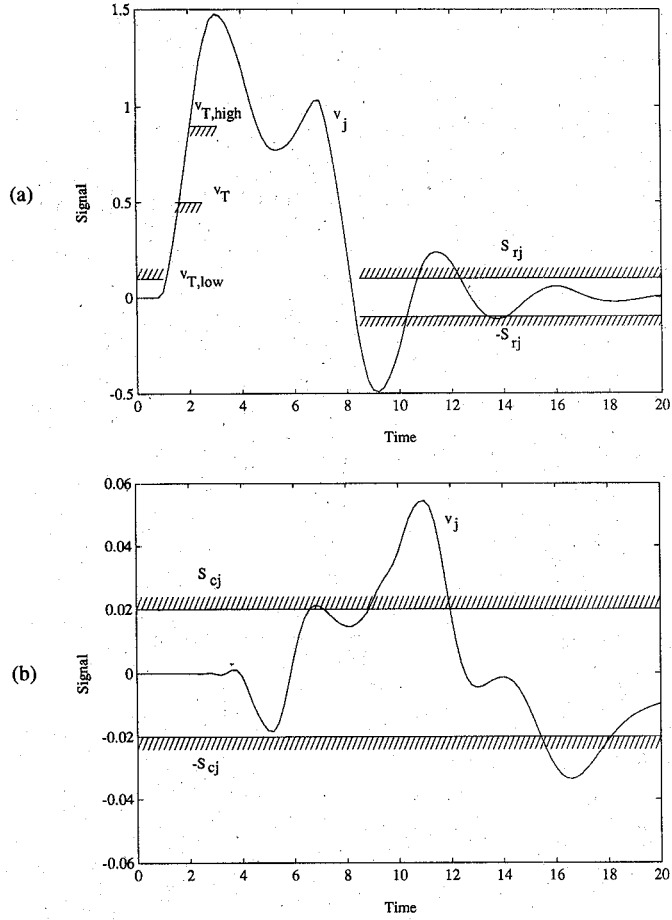


Fig. 2. Examples of specifications for time responses. (a) Signals at nodes  $j, j \subset J_1$ . (b) Signals at nodes  $j, j \subset J_2$ .

subject to

$$g(\phi) \geq 0 \quad (24b)$$

$$h(\phi) = 0 \quad (24c)$$

where  $g(\phi)$  and  $h(\phi)$  represent electrical, physical and geometrical constraints on variables. This is a minimax problem where the maximum of all errors  $e_j, j = 1, 2, \dots, m$ , is minimized. The optimization algorithm we used is a two stage one which combines the robustness of a first-order method of the Gauss-Newton type with the speed of the quasi-Newton method [25]. The optimizer requires user-supplied first order derivatives of  $e$  with respect to  $\phi$ . Such information is obtained by the new approach of sensitivity analysis described in Section II. The optimizer automatically generates approximate second order derivatives by BFGS (Broyden-Fletcher-Goldfarb-Shanno) update to provide fast convergence [25]. At the solution, crosstalk, signal delay and reflections are simultaneously minimized.

#### IV. EXAMPLES

##### Example 1: A 3 Transmission Line Network

Consider the three transmission line system used in [6] and shown in Fig. 3. The excitation is a 6 ns trapezoidal signal shown in Fig. 4.

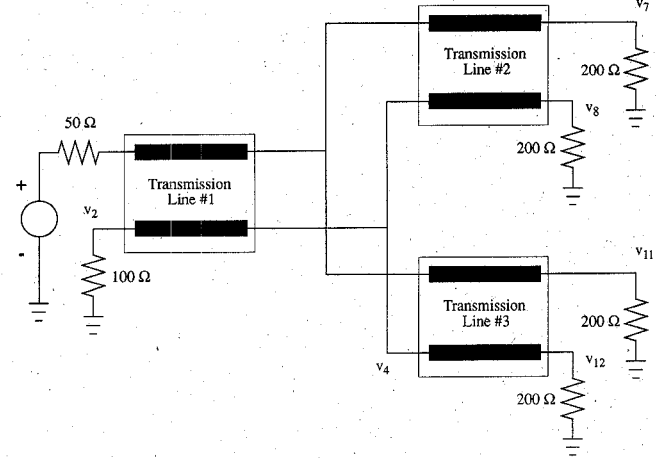


Fig. 3. Circuit schematic for the 3 transmission line network example.

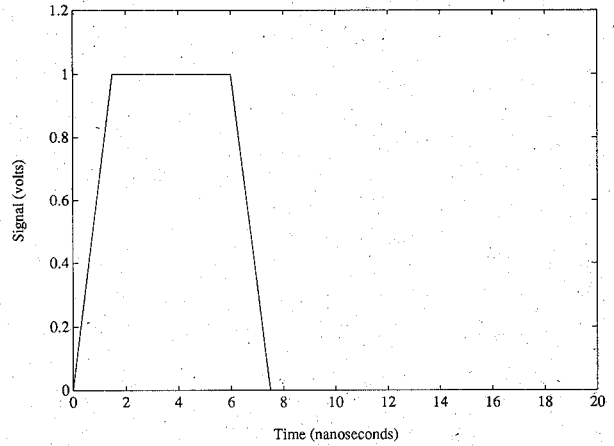


Fig. 4. Trapezoidal signal used as excitation for the 3 transmission line network.

The responses of interest are the signals at nodes 7 and 11 and the crosstalks at nodes 2, 4, 8, and 12. Index sets  $J_1 = \{7, 11\}$  and  $J_2 = \{2, 4, 8, 12\}$ . The responses before optimization are plotted in Fig. 5. The delays of  $v_7$  and  $v_{11}$  are 5.3 ns and 6.1 ns, respectively, based on a threshold of  $v_T = 0.3$  V. We specify that the delay of  $v_7$  and  $v_{11}$  should be reduced to exactly 5.0 ns and 5.1 ns, respectively. A 0.02 V upper specification is imposed on the magnitude of  $v_2, v_4, v_8$  and  $v_{12}$  at 36 time points in the interval [3 ns, 10 ns]. To make the crosstalk and the delay error functions be in comparable scale, we used weighting factors  $w_c = 10$  and  $w_d = 1$ . The total number of error functions is  $m = 292$  where  $e_1(\phi)$  to  $e_4(\phi)$  are defined according to (18) as

$$e_1(\phi) = (v_7(\phi, 5.0 \text{ ns}) - 0.3 \text{ V})$$

$$e_2(\phi) = -(v_7(\phi, 5.0 \text{ ns}) - 0.3 \text{ V})$$

$$e_3(\phi) = (v_{11}(\phi, 5.1 \text{ ns}) - 0.3 \text{ V})$$

$$e_4(\phi) = -(v_{11}(\phi, 5.1 \text{ ns}) - 0.3 \text{ V})$$

and  $e_5(\phi)$  to  $e_{292}(\phi)$  are defined according to (21) as

$$10(v_j(\phi, t_i) - 0.02 \text{ V})$$

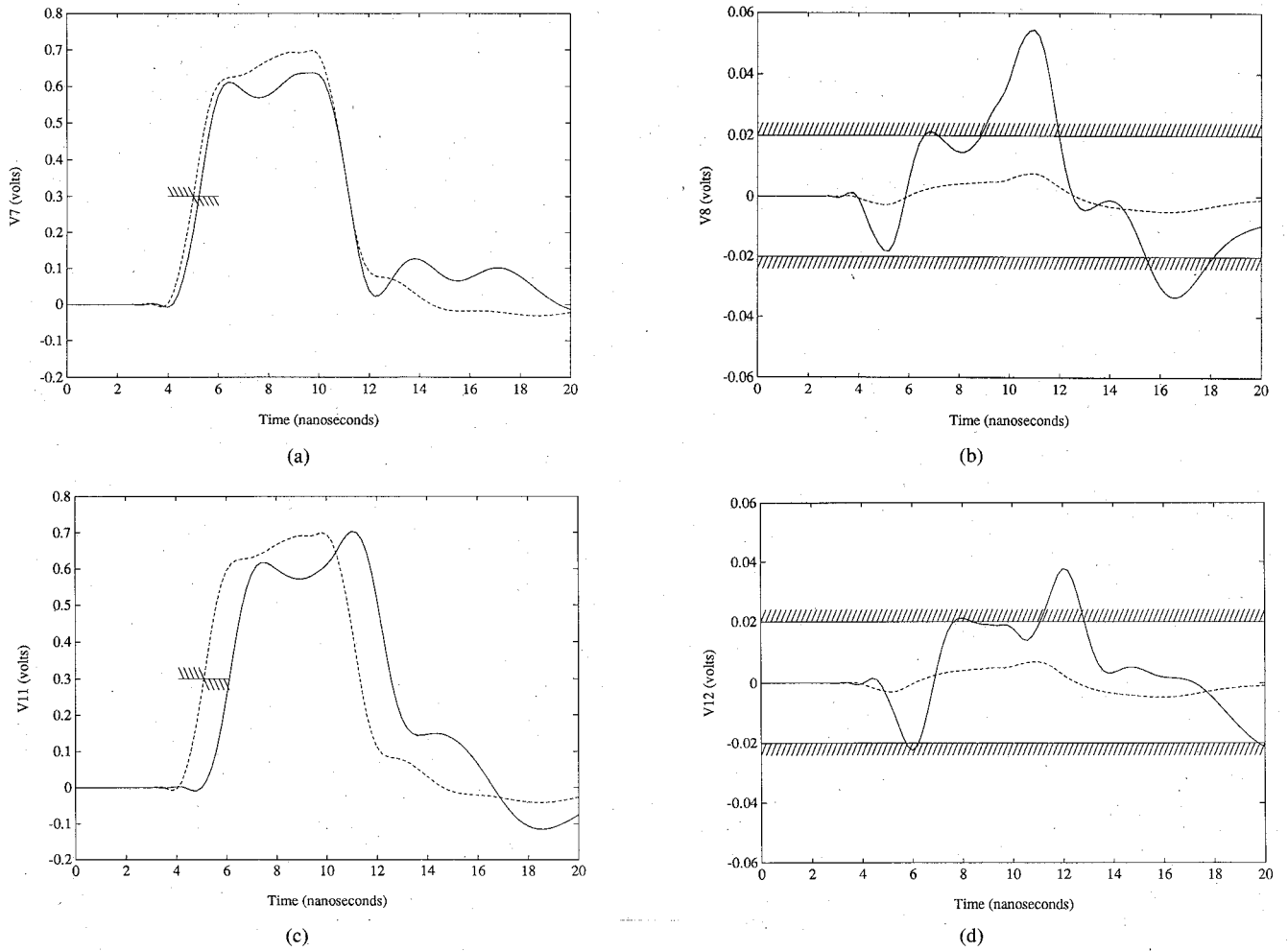


Fig. 5. Signal responses of the circuit of Fig. 3 before (solid line) and after (dashed line) optimization. (a) Signal response  $v_7$ . (b) Crosstalk  $v_8$ . (c) Signal response  $v_{11}$ . (d) Crosstalk  $v_{12}$ .

and

$$-10(v_j(\phi, t_i) + 0.02 \text{ V})$$

for  $j \in \{2, 4, 8, 12\}$  and  $i = 1, 2, \dots, 36$ .

As seen from Fig. 5, all specifications are violated before optimization.

The design variables  $\phi$  include line width  $w$ , distance between the lines  $d$ , circuit board thickness  $h$ , and lengths of the three individual multiconductor lines  $l_1$ ,  $l_2$  and  $l_3$ . Parameters  $w$ ,  $d$  and  $h$  are common among the three transmission line elements. Therefore all the three transmission lines belong to one group. We also require that the total length of the three transmission lines be fixed at 1.34 m and the total width of the two conductors plus the spacing between them be fixed at 0.0025 m. This results in constraints

$$h_1(\phi) = w + d - 0.0025 = 0$$

$$h_2(\phi) = l_1 + l_2 + l_3 - 1.34 = 0.$$

The relative dielectric constant of the circuit board is 4.5. The initial values of the variables are

$$\phi = [w \ d \ h \ l_1 \ l_2 \ l_3]^T = [0.58 \text{ mm} \ 2.49 \text{ mm} \ 1.17 \text{ mm} \ 304.8 \text{ mm} \ 457.2 \text{ mm} \ 609.6 \text{ mm}]^T.$$

During optimization, the transmission line matrix parameters  $\mathbf{R}$ ,  $\mathbf{L}$ ,  $\mathbf{C}$  and  $\mathbf{G}$  are computed from physical parameters using the empirical formulas in [16]. The NILT technique was used to perform network simulation and sensitivity analysis as described in Section II. After 5 iterations of minimax optimization, the objective function of (23) is reduced from 0.266 to  $7.6 \times 10^{-5}$ , approaching the theoretical minimal of 0. The variables after optimization are  $\phi = [w \ d \ h \ l_1 \ l_2 \ l_3]^T = [0.1 \text{ mm} \ 2.4 \text{ mm} \ 0.74 \text{ mm} \ 147.5 \text{ mm} \ 587.6 \text{ mm} \ 604.9 \text{ mm}]^T$ .

Circuit responses after optimization are plotted against those before optimization in Fig. 5. The propagation delay times for  $v_7$  and  $v_{11}$  are reduced to 5.00004 ns and 5.10004 ns, respectively. The magnitude of crosstalk signals  $v_2$ ,  $v_4$ ,  $v_8$  and  $v_{12}$  are all well below the specified 0.02 V level.

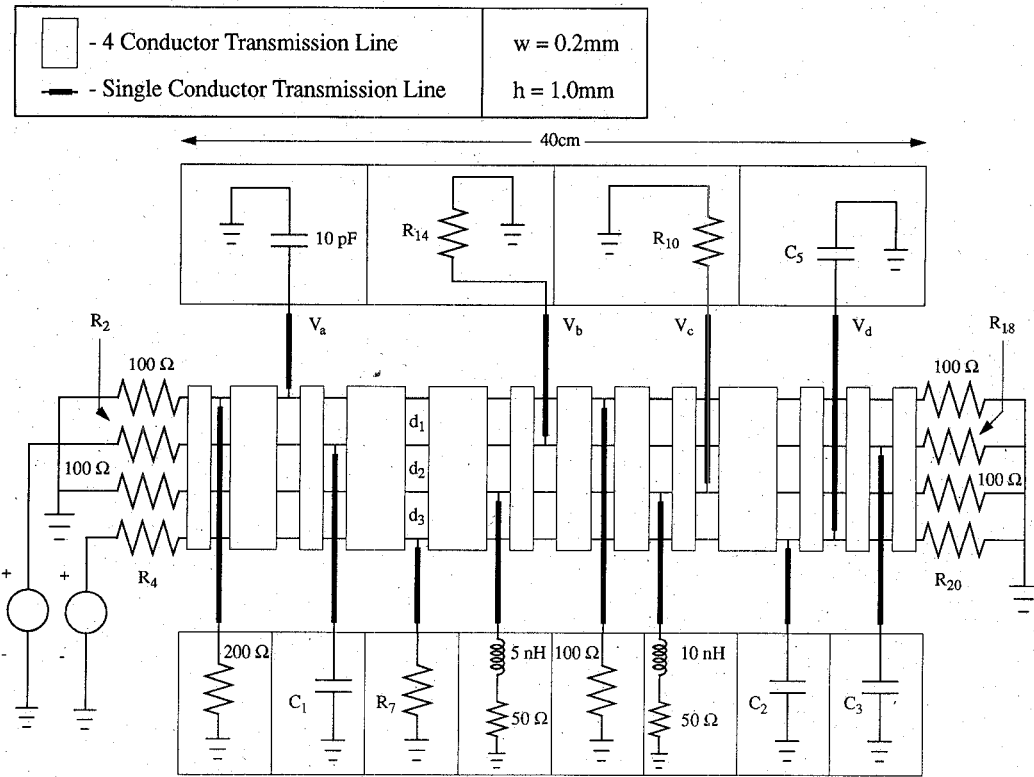


Fig. 6. Circuit diagram for the 25 transmission line network example. There are 13 4-conductor transmission lines and 12 single-conductor transmission lines. Two excitations are simultaneously applied.

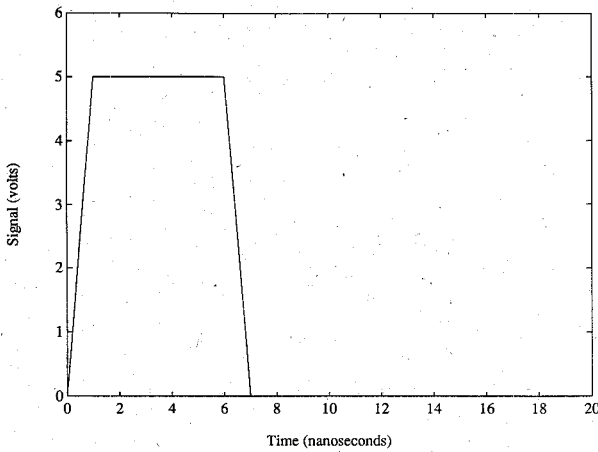


Fig. 7. Trapezoidal signal used as excitation for the circuit of Fig. 6.

#### Example 2: 25 Transmission Line Network

Consider the circuit shown in Fig. 6. The circuit represents a 4-bit bus structure in which the excitation signals propagate through the bus lines to various circuit blocks. There are 13 4-conductor transmission lines and 12 single-conductor transmission lines. The 13 4-conductor transmission lines have the same cross-sectional geometry, being classified into one group. The 12 single-conductor transmission lines form the second group. The circuit contains two excitation sources. The output responses of interest are  $V_a$ ,  $V_b$ ,  $V_c$  and  $V_d$ .  $J_1 = \{b, d\} = J_2 = \{a, c\}$ . The applied voltage of both sources is the

trapezoidal signal shown in Fig. 7. The transient responses of  $V_a$ ,  $V_b$ ,  $V_c$  and  $V_d$  are shown in Fig. 8. The delay times for  $V_b$  and  $V_d$  are approximately 3.1 and 4.1 ns, respectively, based on a 3 V threshold criterion. The crosstalk voltages  $V_a$  and  $V_c$  have peak values being 0.74 V and 0.49 V, respectively.

The specifications for optimization include a 2 ns upper specification on the delay of  $V_b$  and a 4 ns upper specification on the delay of  $V_d$ . Upper specifications were placed on the magnitude of crosstalk voltages  $V_a$  and  $V_c$  at 0.2 V. The weighting factors used were  $w_c = 1$  and  $w_d = 1$ . A specification of 0.2 is also placed on the magnitude of  $V_d$  between the time range of 12.5 ns and 14.5 ns to reduce the reflections in the waveform. The weighting factor  $w_r = 1$ . The total number of error functions is  $m = 61$ . Before optimization all specifications are violated.

The vector of optimization variables  $\phi$  consists of the lengths of the 13 4-conductor transmission lines ( $l_1, l_2, \dots, l_{13}$ ), the distances between the conductors ( $d_1, d_2, d_3$ ), the terminating resistors ( $R_2, R_4, R_7, R_{10}, R_{14}, R_{18}, R_{20}$ ), and the terminating capacitors ( $C_1, C_2, C_3, C_5$ ). These variables are also described in Table I. The total number of variables is 27.

The minimum distance separating the conductors was set at 0.8 mm while the maximum total separation between conductors 1 and 4 was set at 5 mm. The total length of the 13 transmission lines was fixed at 40 cm.

The initial value of the overall objective function (23) was 1.717. After 10 iterations of optimization the value

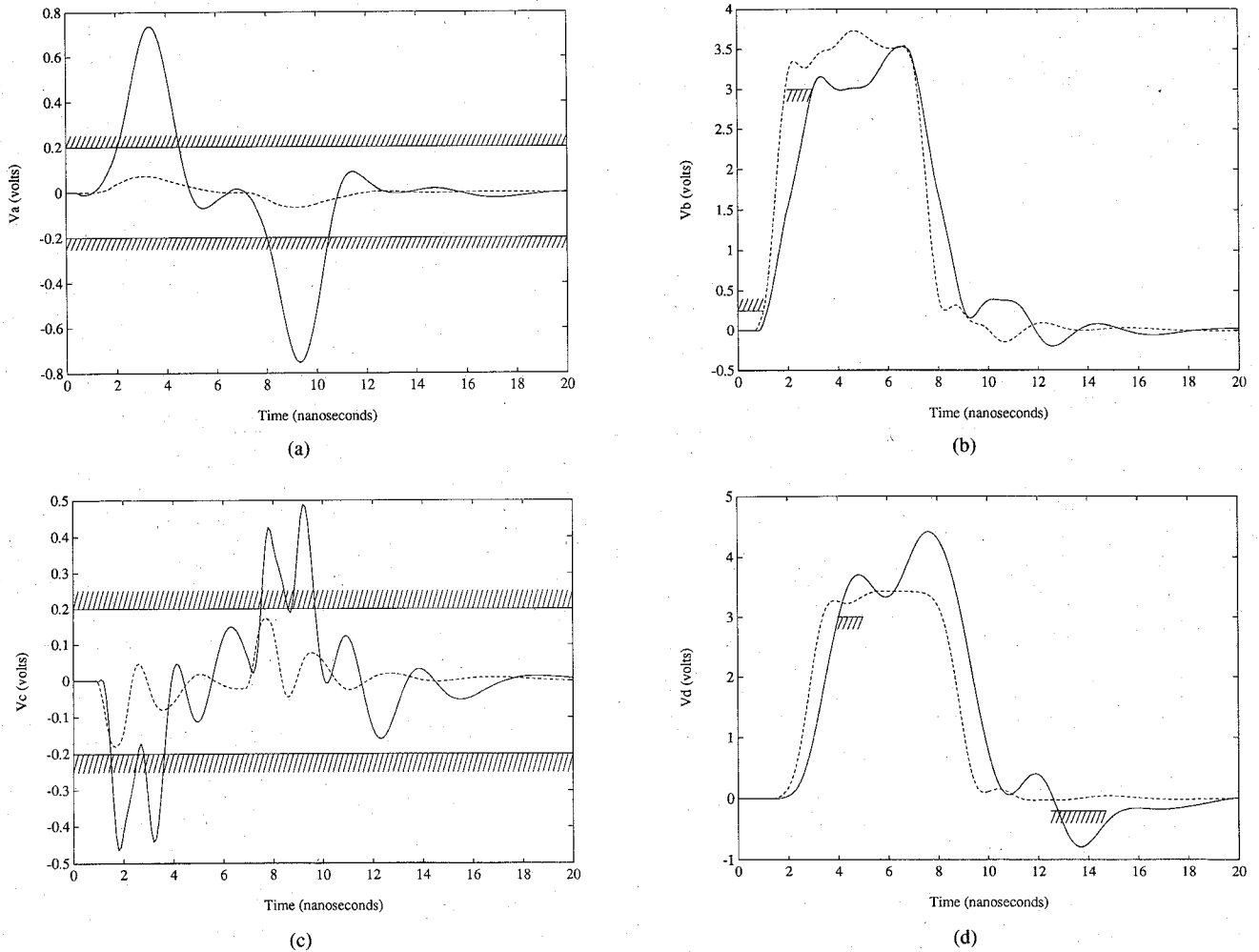


Fig. 8. The 25 transmission line example. Response before (solid line) and after (dashed line) optimization. (a) Crosstalk  $V_a$ . (b) Signal response  $V_b$ . (c) Crosstalk  $V_c$ . (d) Signal response  $V_d$ .

TABLE I  
OPTIMIZATION VARIABLES FOR EXAMPLE 2

Variable	Before Opt.	After Opt.	Variable	Before Opt.	After Opt.
$l_1$	0.025 m	0.0531 m	$d_1$	1.0 mm	3.3 mm
$l_2$	0.035 m	0.0349 m	$d_2$	1.0 mm	0.86 mm
$l_3$	0.025 m	0.0288 m	$d_3$	1.0 mm	0.84 mm
$l_4$	0.04 m	0.014 m	$R_2$	25 $\Omega$	24.91 $\Omega$
$l_5$	0.04 m	0.01 m	$R_4$	25 $\Omega$	24.5 $\Omega$
$l_6$	0.025 m	0.01 m	$R_7$	200 $\Omega$	164.61 $\Omega$
$l_7$	0.035 m	0.0163 m	$R_{10}$	200 $\Omega$	28.52 $\Omega$
$l_8$	0.035 m	0.0178 m	$R_{14}$	100 $\Omega$	254.84 $\Omega$
$l_9$	0.025 m	0.0379 m	$R_{18}$	100 $\Omega$	85.04 $\Omega$
$l_{10}$	0.04 m	0.0692 m	$R_{20}$	100 $\Omega$	75.73 $\Omega$
$l_{11}$	0.025 m	0.0166 m	$C_1$	5 pF	0.1 pF
$l_{12}$	0.025 m	0.0367 m	$C_2$	5 pF	0.1 pF
$l_{13}$	0.025 m	0.0548 m	$C_3$	5 pF	0.1 pF
			$C_5$	10 pF	8.1 pF

was reduced to  $-0.143$ , all the specifications being satisfied. The parameters before and after optimization are listed in Table I. The output responses  $V_a$ ,  $V_b$ ,  $V_c$  and  $V_d$  after optimization are plotted against those before optimi-

mization in Fig. 8. The propagation delay of  $V_b$  and  $V_d$  are reduced to 2 ns and 3.5 ns, respectively. The peaks of crosstalk voltages  $V_a$  and  $V_c$  are reduced to 0.07 and 0.17 V, respectively. In addition, the reflections in the output response  $V_d$  were significantly smaller than before optimization. The rise/fall times of signal  $V_b$  were also improved.

## V. CONCLUSION

High-speed VLSI interconnect design using distributed multiconductor transmission line models is carried out by time-domain optimization. Minimization of transmission line effects such as crosstalk, delay and reflection is formulated into a minimax optimization problem. The NILT technique for multiconductor transmission lines is expanded to directly address the VLSI interconnect environment, resulting in increased efficiency for simulation and sensitivity analysis. Powerful gradient based minimax optimization, integrated with the proposed exact sensitivity analysis technique, demonstrates the feasibility and practicality of the physical/geometrical oriented interconnect

design. The technique developed is an important step towards overall optimal design of high-speed VLSI systems.

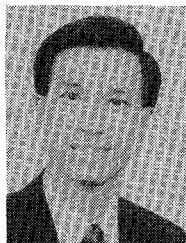
#### ACKNOWLEDGMENT

Technical discussions with Dr. S. Daijavad of IBM T. J. Watson Research Center, Yorktown Heights, New York, is appreciated. The first author also thanks Dr. J. W. Bandler of McMaster University, Hamilton, Canada, for his support during the initial stages of this work.

#### REFERENCES

- [1] R. Griffith and M. S. Nakhla, "Time-domain analysis of lossy coupled transmission lines," *IEEE Trans. Microwave Theory Tech.*, vol. 38, pp. 1480-1487, 1990.
- [2] S. Lum, M. S. Nakhla, and Q. J. Zhang, "Sensitivity analysis of lossy coupled transmission lines," *IEEE Trans. Microwave Theory Tech.*, vol. 39, pp. 2089-2099, 1991.
- [3] R. A. Sainati and T. J. Moravec, "Estimating high speed circuit interconnect performance," *IEEE Trans. Circuits Syst.*, vol. 36, pp. 533-541, 1989.
- [4] H. Hasegawa and S. Seki, "Analysis of interconnection delay on very high-speed LSI/VLSI chips using a microstrip line model," *IEEE Trans. Electron Devices*, vol. ED-31, pp. 1954-1960, 1984.
- [5] A. R. Djordjevic, T. K. Sarkar, and R. F. Harrington, "Time-domain response of multiconductor transmission lines," *Proc. IEEE*, vol. 75, pp. 743-764, 1987.
- [6] A. R. Djordjevic and T. K. Sarkar, "Analysis of time response of lossy multiconductor transmission line networks," *IEEE Trans. Microwave Theory Tech.*, vol. MTT-35, pp. 898-908, 1987.
- [7] O. A. Palusinski and A. Lee, "Analysis of transients in nonuniform and uniform multiconductor transmission lines," *IEEE Trans. Microwave Theory Tech.*, vol. 37, pp. 127-138, 1989.
- [8] F. Y. Chang, "The generalized method of characteristics for waveform relaxation analysis of lossy coupled transmission lines," *IEEE Trans. Microwave Theory Tech.*, vol. 37, pp. 2028-2038, 1989.
- [9] S. S. Gao, A. Y. Yang, and S. M. Kang, "Modelling and simulation of interconnection delays and crosstalk in high-speed integrated circuits," *IEEE Trans. Circuits Syst.*, vol. 37, pp. 1-9, 1990.
- [10] M. S. Nakhla, "Analysis of pulse propagation on high-speed VLSI chips," *IEEE J. Solid-State Circuits*, vol. 25, pp. 490-494, 1990.
- [11] K. Kiziloglu, N. Dagli, G. L. Matthaei, and S. I. Long, "Experimental analysis of transmission line parameters in high-speed GaAs digital circuit interconnects," *IEEE Trans. Microwave Theory Tech.*, vol. 39, pp. 1361-1367, 1991.
- [12] D. Winklestein, M. B. Steer and R. Pomerleau, "Simulation of arbitrary transmission line networks with nonlinear terminations," *IEEE Trans. Circuits Syst.*, vol. 38, pp. 418-422, 1991.
- [13] T. Tang and M. S. Nakhla, "Analysis of high-speed VLSI interconnects using the asymptotic waveform evaluation technique," *IEEE Trans. Computer-Aided Design*, vol. 11, pp. 341-352, 1992, to be published.
- [14] A. E. Ruehli, "Inductance calculations in a complex integrated circuits environment," *IBM J. Research Dev.*, vol. 16, pp. 470-481, 1972.
- [15] A. R. Djordjevic, R. F. Harrington, and T. K. Sarkar, *Matrix Parameters of Multiconductor Transmission Lines*. Boston: Artech House, 1989.
- [16] C. S. Walker, *Capacitance, Inductance and Crosstalk Analysis*. Boston: Artech House, 1990.
- [17] C. W. Ho, A. E. Ruehli and P. A. Brennan, "The modified nodal approach to network analysis," *IEEE Trans. Circuits Syst.*, vol. CAS-22, pp. 504-509, 1975.
- [18] S. W. Director and R. A. Rohrer, "Automated network design-the frequency domain case," *IEEE Trans. Circuit Theory*, vol. CT-16, pp. 330-337, 1969.
- [19] J. W. Bandler and Q. J. Zhang, "Optimization techniques for modelling, diagnosis and tuning," in *Analog Methods for Computer-Aided Circuit Analysis and Diagnosis*, T. Ozawa, Ed. New York: Marcel Dekker, 1988, ch. 14.
- [20] J. W. Bandler and S. H. Chen, "Circuit optimization: the state-of-the-art," *IEEE Trans. Microwave Theory Tech.*, vol. 36, pp. 424-443, 1988.
- [21] W. Nye, D. C. Riley, A. Sangiovanni-Vincentelli and A. L. Tits, "DELIGHT-SPICE: An optimization-based system for the design of integrated circuits," *IEEE Trans. Computer-Aided Design*, vol. 7, pp. 501-519, 1988.
- [22] J. W. Bandler, "Computer-aided circuit optimization," in *Modern Filter Theory and Design*, G. C. Temes and S. K. Mitra, Eds. New York: Wiley-Interscience, 1973, chap. 6.
- [23] L. O. Chua and P. M. Lin, *Computer-Aided Analysis of Electronic Circuits*. Englewood Cliffs, NJ: Prentice-Hall, 1975.
- [24] D. A. Calahan, *Computer-Aided Network Design*, 2nd ed. New York: McGraw-Hill, 1972.
- [25] J. W. Bandler, W. Kellermann, and K. Madsen, "A superlinearly convergent minimax algorithm for microwave circuit design," *IEEE Trans. Microwave Theory Tech.*, vol. 33, pp. 1519-1530, 1985.

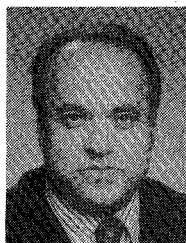
**Qi-Jun Zhang** (S'84-M'87), for photograph and biography, see this issue, p. 1400.



interconnects.

**Stephen Lum** (S'90-M'92) received the B.A.Sc. degree in electrical engineering from the University of Waterloo, Waterloo, Canada in 1988 and the M.Eng. degree from Carleton University, Ottawa, ON Canada, in 1991.

He is currently a member of the Scientific Staff at Bell-Northern Research providing applications support in the areas of high-speed circuit simulation signal integrity and electromagnetic compatibility. His research interests include simulation and computer-aided design of high-speed VLSI



**Michel S. Nakhla** (S'73-M'76-SM'88) received the B.Sc. degree in electronics and communications from Cairo University, Egypt in 1967 and the M.A.Sc. and Ph.D. degrees in electrical engineering from Waterloo University, ON, Canada in 1973 and 1975, respectively.

During 1975, he was a Postdoctoral Fellow at University of Toronto, Ontario, Canada. In 1976 he joined Bell-Northern Research, Ottawa, ON Canada, as a member of the Scientific Staff where he became manager of the simulation group in 1980 and manager of the computer-aided engineering group in 1983. In 1988, he joined Carleton University, Ottawa, where he is currently a Professor in the Department of Electronics. His research interests include computer-aided design of VLSI and communication systems, high-frequency interconnects and synthesis of analog circuits.

Dr. Nakhla was the recipient of the Bell-Northern Research Outstanding Contribution Patent Award in 1984 and in 1985. Currently he is the holder of the Computer-Aided Engineering Industrial Chair established at Carleton University by Bell Northern Research and the Natural Sciences and Engineering Research Council of Canada.